ACS chemical biology

Articles

pubs.acs.org/acschemicalbiology

S-Glutathionylation at Cys328 and Cys542 Impairs STAT3 Phosphorylation

Elena Butturini,[†] Elena Darra,[†] Giulia Chiavegato,[†] Barbara Cellini,[†] Flora Cozzolino,[‡] Maria Monti,[‡] Piero Pucci,[‡] Daniele Dell'Orco,[†] and Sofia Mariotto*[,†]

[†]Department of Life and Reproduction Sciences, Biochemistry Section, University of Verona, Verona 37134, Italy

[‡]CEINGE Biotecnologie Avanzate and Department of Chemical Science, University of Naples "Federico II", Naples 80138, Italy

Supporting Information

ABSTRACT: STAT3 is a latent transcription factor that promotes cell survival and proliferation and is often constitutively active in cancers. Although many reports provide evidence that STAT3 is a direct target of oxidative stress, its redox regulation is poorly understood. Under oxidative conditions STAT3 activity can be modulated by S-glutathionylation, a reversible redox modification of cysteine residues. This suggests the possible cross-talk between phosphorylation and glutathionylation and points out that STAT3 is susceptible to redox regulation. Recently, we reported that decreasing the GSH content in different cell lines induces inhibition of STAT3 activity through the reversible oxidation of thiol groups. In the present work, we demonstrate that GSH/diamide treatment induces S-glutathionylation of STAT3 in the recombinant purified form. This effect was completely reversed by treatment with the reducing agent dithiothreitol, indicating that S-glutathionylation of STAT3 was related to formation of protein-mixed disulfides. Moreover, addition of the bulky negatively charged GSH moiety impairs JAK2-mediated STAT3 phosphorylation, very likely interfering with tyrosine accessibility and thus affecting protein structure and function. Mass mapping analysis identifies two glutathionylated cysteine residues, Cys328 and Cys542, within the DNA-binding domain and the linker domain, respectively. Site direct mutagenesis and *in vitro* kinase assay confirm the importance of both cysteine residues in the complex redox regulatory mechanism of STAT3. Cells expressing mutant were resistant in this regard. The data presented herein confirmed the occurrence of a redox-dependent regulation of STAT3, identified the more redox-sensitive cysteines within STAT3 structure, and may have important implications for development of new drugs.

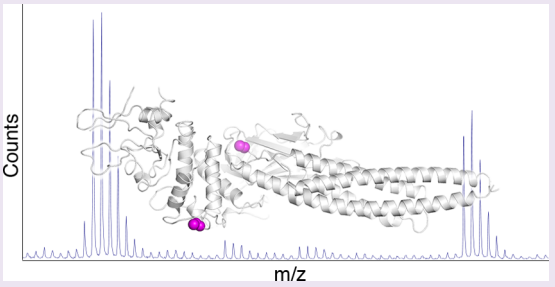

Signal transducer and activator of transcription 3 (STAT3α) is a member of a family of seven proteins that relay signals from activated cytokine and growth factor receptors in the plasma membrane to the nucleus, where they regulate gene transcription.[1,2] All mammalian STAT proteins (STAT 1, 2, 3, 4, 5A, 5B, 6) share six structural regions: an N-terminal domain (NT), a coiled-coil domain (CCD), a DNA-binding domain (DBD), linker domain (LD), a Src homology 2 domain (SH2), and a transcription activation domain (TAD) at the carboxy terminus (Figure 1).[3,4]

Multiple distinct steps are involved within the STAT3 signaling pathway; upon extracellular receptor stimulation by growth factors or cytokines, the receptor dimerizes, triggering the activation of the Janus protein tyrosine kinases (JAKs), which are associated with the cytoplasmic tail of the receptor. Activated JAKs phosphorylate recruited STAT3 proteins at a specific tyrosine (Tyr705), and the phosphorylated STAT3 monomers dissociate from the receptor to form dimers that translocate from the cytoplasm to the nucleus, where they bind to target DNA motifs.[5,6] Binding of STAT3 to a specific DNA domain promotes the expression of a large variety of genes encoding mediators crucial for the classic physiological acute phase response or involved in a variety of critical cells functions, including differentiation, proliferation, apoptosis, angiogenesis, metastasis, and immune responses.[7−9]

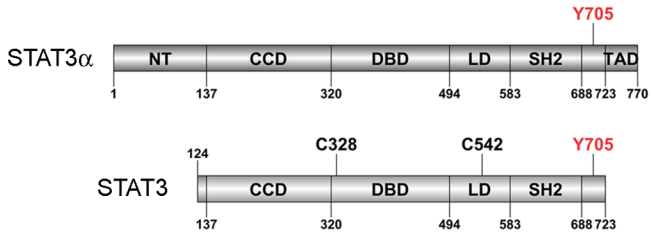

Figure 1. Domain structure of STAT3. The six domains of STAT3α are N-domain (NT), coiled-coil domain (CCD), DNA-binding domain (DBD), linker domain (LD), a Src homology 2 domain (SH2), and transcriptional activation domain (TAD). Between SH2 and TAD there is a tail segment that contains the phosphorylation site Y705. The construct used comprises residues 124−723 and lacks the N-terminal cooperativity domain as well as the C-terminal trans-activation domain.

Received: January 27, 2014
Accepted: June 18, 2014
Published: June 18, 2014

   dx.doi.org/10.1021/cb500407d | *ACS Chem. Biol.* 2014, 9, 1885−1893

Although STAT3 activation normally leads to the physiological response, deregulation of this transduction cascade could lead to tissue damage and could be directly or indirectly involved in different inflammation-correlated diseases.[10−14] Furthermore, STAT3 is considered as an oncoprotein, and its constitutive activation is described in a variety of human cancers.[4,15,16] A large body of evidence suggests that constitutively active STAT3 induces deregulation of growth and survival, promotion of angiogenesis, and suppression of host's immune surveillance of tumor. Moreover, aberrant STAT3 promotes invasion and metastasis, thereby contributing to tumor progression. Thus, inhibition of aberrant STAT3 activity by genetic or pharmacological approaches induces growth arrest and apoptosis of tumor cells *in vitro* as well as tumor regression *in vivo*, validating STAT3 as a suitable molecular target for anticancer drug discovery.[4,15,17]

Several lines of evidence suggest that STAT3 activation is susceptible to redox regulation. Although reactive oxygen species (ROS) trigger tyrosine phosphorylation and up-regulate the DNA-binding activity of STAT3,[18−21] otherwise divergent reports indicate that ROS are able to induce oxidation of conserved cysteines in the DNA-binding domain of STAT3, hindering its transcriptional activity.[22,23] In addition, it has been shown that pretreatment of microvascular endothelial cells with nitrosocyclohexyl acetate, a nitroxyl (HNO) donor, inhibits STAT3 phosphorylation through the formation of sulfenic acid at the cysteine residues.[24] In this regard, other reports demonstrated that protein sulfenic acids are intermediate stage in the oxidation of cysteine and are able to react with glutathione (GSH) or glutathione disulfide (GSSG), resulting in protein glutathionylation.[25−27] Hence, regulation of STAT3 by ROS is a complex and poorly defined process.

Redox-sensitive proteins exhibit a striking differential susceptibility to ROS; while a protein may contain numerous cysteine residues, only a minority of these will have the chemical properties to function as possible target sites for oxidants. This is largely due to the reactivity of anionic sulfur to various oxidizing agents.

Mild oxidative stress may induce reversible modifications, including the S-glutathionylation of cysteine residues.[28] This reaction may have a dual role: protection from irreversible damage and modulation of protein function. Conversely, excessive oxidative stress triggers irreversible modification of thiol groups of proteins generally associated with permanent loss of function, misfolding, and aggregation.[29−31] It has been demonstrated that STAT3 can be S-glutathionylated in HepG2 cells under oxidative conditions with concomitant inhibition of phosphorylation, thus suggesting the possible cross-talk between these two post-translational reactions.[32]

Recently, we reported that decrease in GSH content in different cell lines induces inhibition of STAT3 activity through the reversible oxidation of thiol groups. Perturbation of the intracellular GSH/GSSG homeostasis is involved in the induction of reversible S-glutathionylation of STAT3 with concomitant decrease in Tyr705 phosphorylation, pointing out that this signal transcription factor is susceptible to redox regulation.[33,34]

In this report we demonstrate S-glutathionylation of STAT3 in the recombinant purified form and identify the cysteine residues mainly involved in this reaction. Furthermore, we confirm that this post-translational modification impairs JAK2-mediated STAT3 tyrosine phosphorylation, possibly interfering with tyrosine accessibility, suggesting that S-glutathionylation may represent a mechanism of STAT3 activity regulation in cells.

Moreover, we evaluate the importance of identified cysteine residues in S-glutathionylation of STAT3 in a cellular environment using HeLa cells transfected with STAT3 mutant.

RESULTS AND DISCUSSION

S-Glutathionylation, a redox-based modification of proteins thiols, has recently emerged as an important signaling mechanism in physiological and pathological conditions.[35] Many reports provide evidence that STAT3 is a direct target of oxidative stress, and indicate that glutathionylation might represent the key event in redox STAT3 modulation.

Diamide and Glutathione Treatment Inhibit STAT3 Phosphorylation. To determine the effect of oxidative stress on glutathionylation of STAT3, 50 ng of recombinant protein was incubated with different thiol-specific oxidants for 15 min and analyzed with anti-GSH antibody under non-reducing condition.

As shown in Figure 2A, treatment of STAT3 with GSH, GSSG, or diamide alone did not cause significant modification of the protein. However, when STAT3 underwent to a combined treatment with 100 μM diamide and 125 μM GSH, S-glutathionylation of the protein was rapidly observed. This modification was completely reversed by the subsequent addition of 20 mM DTT for 10 min. Western blot exhibited equivalent STAT3 levels in all samples (Figure 2A).

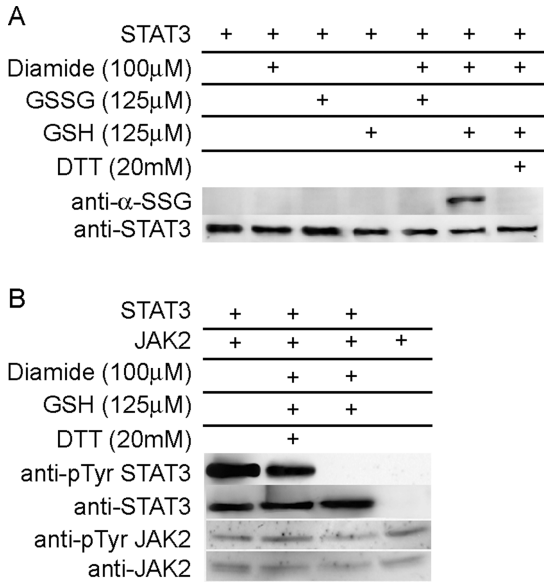

Figure 2. Effect of diamide/GSH treatment on S-glutathionylation and phosphorylation of STAT3. (A) Western blot analysis under non-reducing conditions shows that only diamide/GSH combined treatment induced STAT3 S-glutathionylation. This post-translational modification was completely reversed by DTT treatment. The blot exhibits equivalent STAT3 levels in all samples. (B) In vitro JAK2 kinase assay was performed using JAK2 active protein and STAT3. Western blot analysis shows that JAK2 induced STAT3 Tyr705 phosphorylation, a prerequisite for STAT3 functionality. On the other hand, the anti-pTyr705 STAT3 antibody was not able to recognize protein after diamide/GSH treatment. The blots exhibit equivalent STAT3 and JAK2 protein levels in all samples. The images are representative of 4 independent experiments.

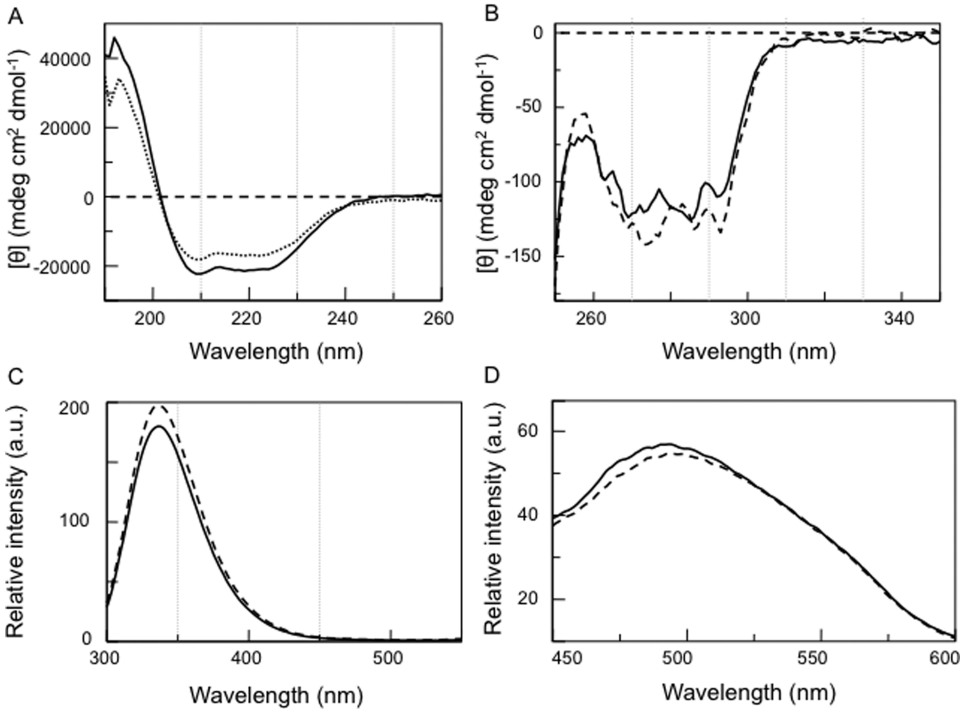

Figure 3. Spectral properties of recombinant purified STAT3 in the glutathionylated (- - -) and non-glutathionylated (—) form. (A) Far-UV CD spectra registered at 0.1 mg mL^{-1} protein concentration. (B) near-UV CD spectra registered at 0.5 mg mL^{-1} protein concentration. (C) Intrinsic fluorescence emission spectra (λ_{exc} = 280 nm) registered at 0.1 mg mL^{-1} protein concentration. (D) ANS emission fluorescence spectra (λ_{exc} = 365 nm) registered at 0.1 mg mL^{-1} protein concentration. All measurements were performed in 20 mM Tris-HCl, pH 7.5 at 25 °C.

Since STAT3 was glutathionylated in the presence of oxidants, we examined whether this modification might affect STAT3 phosphorylation. Phosphorylation of both STAT3 and S-glutathionylated STAT3 was analyzed by *in vitro* kinase assay. In the presence of JAK2, STAT3 protein exhibited an increased level of phosphorylation at Tyr705, a prerequisite for STAT3 functionality. Figure 2B shows that treatment with 100 μM diamide and 125 μM GSH significantly decreased the level of STAT3 tyrosine phosphorylation. Addition of 20 mM DTT before JAK2 incubation almost completely rescued STAT3 phosphorylation level (Figure 2B). Western blot analysis exhibited equivalent STAT3 and JAK2 protein levels in all samples (Figure 2B).

In vitro kinase assay confirms that S-glutathionylation of STAT3 transiently prevents Tyr705 phosphorylation. The molecular mechanism of this event is still unknown and deserves to be deeply investigated. One possibility is that S-thiolation of STAT3 might hamper recognition of the Tyr705 region by JAK2.

Because the addition of GSH, a bulky negatively charged group, might alter protein structure and consequently function, in a manner similar to the addition of a phosphate, the effect of S-glutathionylation on the secondary and tertiary structure of STAT3 were evaluated by fluorescence and CD spectroscopy. The CD spectrum of purified recombinant STAT3 in the far-UV region shows the typical aspect of a high α-helix content protein with two minima at 208 and 222 nm (Figure 3A, —). The estimated secondary structure content, reported in Table 1, corresponds reasonably well to that deduced from the three-dimensional structure of the protein.[36] In the near-UV region, STAT3 displays a broad negative dichroic band at 270−290 nm, indicative of the asymmetry of aromatic amino acids (Figure 3B, —). When excited at 280 nm, the protein shows an intrinsic fluorescence emission maximum at 336 nm, typical of aromatic amino acids in an apolar environment (Figure 3C, —). Finally, in the presence of STAT3, the ANS emission fluorescence maximum shifts from 515 to 493, thus indicating the presence of exposed hydrophobic patches in the native protein (Figure 3D, —). These data indicate that purified recombinant STAT3 is present *in vitro* in a folded conformation easily recognized by JAK2, confirming the results obtained by the *in vitro* kinase assay.

Table 1. Secondary Structure Content of Recombinant Purified STAT3 in Non-glutathionylated or S-Glutathionylated form[a]

	α-helix	β-structure	random coil
non-glutathionylated STAT3	67.4	14.9	17.7
S-glutathionylated STAT3	54.3	20.2	25.5

[a]The values are expressed in percentage.

Comparison of the far-UV CD spectrum (Figure 3A) and the secondary structure content (Table 1) of S-glutathionylated STAT3 with native STAT3 reveals that S-glutathionylation leads to a reduction in the α-helix content and an increase in both the β-structure and random coil content. Moreover, small changes can be observed in the near-UV CD spectrum of S-glutathionylated STAT3 (Figure 3B, - - -), in the 255−260 and 280−285 nm regions.

S-Glutathionylation does not significantly change the intrinsic fluorescence emission spectrum of the protein (Figure 3C, - - -) but induces a 5 nm red-shift of the ANS-emission spectrum with respect to native STAT3 (Figure 3D, - - -). These data indicate that S-glutathionylation causes subtle conformational changes involving aromatic amino acids (mostly

dx.doi.org/10.1021/cb500407d | *ACS Chem. Biol.* 2014, 9, 1885−1893

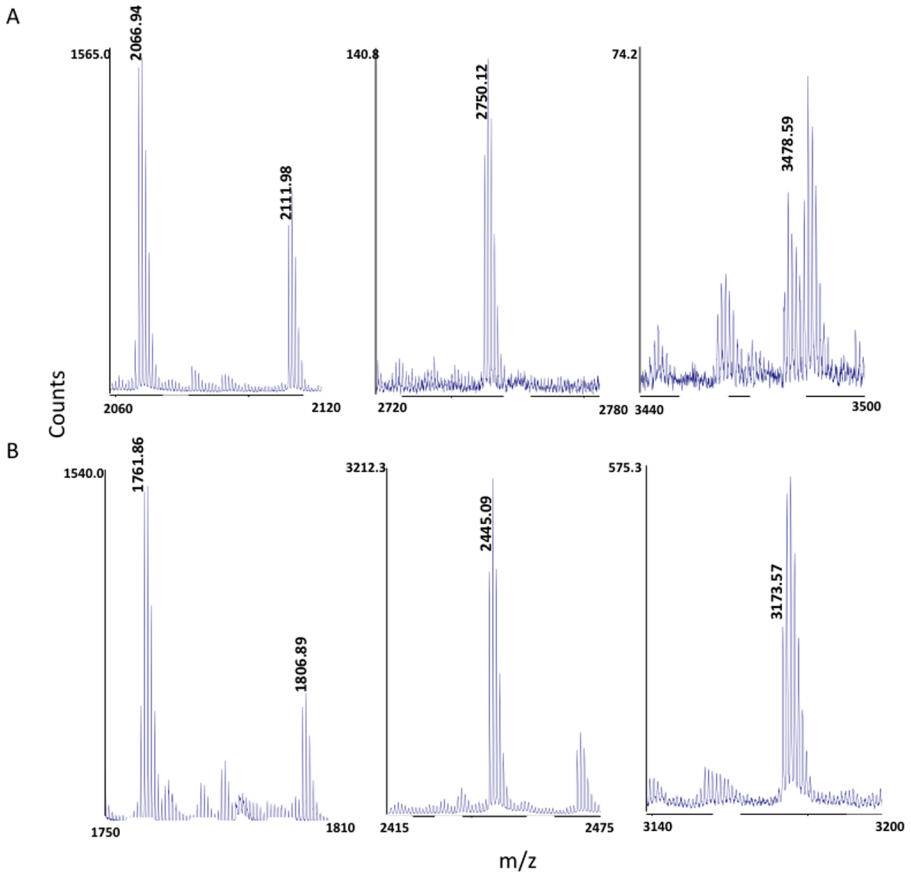

Figure 4. Partial MALDI-MS spectra of the tryptic digest from gluthationylated STAT3. (A) Mass signals associated to the putative modified peptides 326−340, 532−548, 686−707, and 424−451, respectively. (B) Mass signals recorded following incubation with DTT.

tyrosine and phenylalanine residues), leading to a slightly decreased exposure of hydrophobic surfaces.

Cys328 and Cys542 within STAT3 Protein Are Targets for S-Glutathionylation. Despite glutathionylation being described in many proteins, only in some cases have the modification sites been identified. Two major factors are involved in determining the susceptibility of thiols toward redox regulation, the accessibility of the thiol itself within the three-dimensional structure of the protein and the reactivity of the cysteine, which is dependent on neighboring amino acids.[37,38]

STAT3 possesses 12 cysteines, which are potential targets for S-glutathionylation. In order to identify the more sensitive cysteine residues, an aliquot of glutathionylated STAT3 was desalted by RP-HPLC, dissolved in ammonium bicarbonate, and digested with trypsin. The resulting peptide mixture was directly analyzed by MALDI-MS. Most of the mass signals in the spectra could be mapped onto the anticipated sequence of recombinant STAT3 leading to coverage of about 80% of the amino acid sequence. The results are summarized in Supporting Table 1.

The mass signals at m/z 3478.6, 2750.1, 2111.9, and 2066.9 could not be assigned to any peptide within the STAT3 sequence and were then putative candidates for modification (Figure 4A). On the basis of their unique mass value, these peaks were assigned to S-glutathionylated species, corresponding to the 424−451, 686−707, 532−548, and 326−340 peptides, containing cysteine residues at position 426, 687, 542, and 328, respectively. The contemporaneous presence in the spectra of the mass signals at m/z 3173.5 and 2445.1 corresponding to the unmodified forms of the 424−451 and 686−707 peptides suggested that only a partial modification of Cys426 and Cys687 had occurred (Supporting Table 1). On the contrary, the mass signals corresponding to the unmodified forms of the peptides 532−548 and 326−340 were negligible, indicating that Cys542 and Cys328 had been completely S-glutathionylated. These assignments were confirmed by incubating the peptide mixture with DTT and reanalysing the sample by MALDI-MS. All of the signals corresponding to putative GSH-modified peptides disappeared in the spectra, giving rise to peaks corresponding to the expected unmodified peptides at m/z 3173.5, 2445.1, 1806.9, and 1761.9, respectively (Figure 4B).

The signals corresponding to S-glutathionylated peptides were also submitted to MS/MS experiments further confirming the modification state of the Cys residues. As an example, Figure 5 shows the MALDI-MS/MS spectrum of the ion at m/z 2066.9 exhibiting the almost complete series of y ions confirming the assignment to the 326−340 peptide. The y ion pairs at m/z 1841.8 and 1433.7 unambiguously demonstrated the presence of a S-glutathionylated Cys residue at position 328.

Computing the solvent accessible surface area (ASA) for the two residues based on the available crystallographic structure of the STAT3 monomer (PDB entry: 1BG1)[39] highlighted significant differences among the two cysteine residues. Cys542 is significantly solvent-exposed (ASA = 41.8 Å^2), while Cys328 is essentially buried, showing lower ASA value (9.3 Å^2). Glutathionylation of Cys542 may be stabilized by interactions with the polar side chains of Gln543 and Asn538,

dx.doi.org/10.1021/cb500407d | ACS Chem. Biol. 2014, 9, 1885−1893

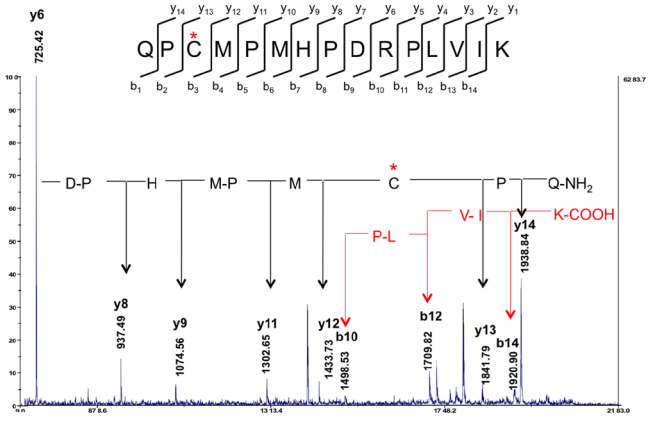

Figure 5. Partial MALDI-MS/MS spectrum of the ion at m/z 2066.9 corresponding to the peptide 326−340. The presence of several daughter ions belonging to the y and b series confirms the peptide sequence (see insert). The daughter ion at m/z 1433.73 (y12) demonstrates the presence of gluthationylated Cys328 indicated with an asterisk in the inset.

which will likely perturb the interaction between helix 501−515 and helix 521−532 mediated by the hydrophobic residues Trp501, L533, and Tyr539. On the other hand, the introduction of a bulky GSH group in the narrow cleft containing Cys328 would locally affect the loop conformation as well as pull apart the 321−325 β-strand and the 198−252 helix in the coiled-coil domain, with consequences that may extend to the overall interface between the coiled-coil domain and the DNA-binding domain (Figure 6). Indeed, CD and fluorescence spectroscopy data indicate that S-glutathionylation of STAT3 induces slight changes of the secondary and tertiary structure of the protein, in line with the structural inferences by crystallographic data. Although the 3D structure of glutathionylated STAT3 is not available, it can be speculated that the small conformational change induced by GSH addition could in turn induce a conformational change in the phosphorylation site, thus justifying the loss of a productive STAT3−JAK2 interaction.

The biological role of the identified modified cysteines was evaluated by generating single or double site-specific mutants in which each of the two cysteines was substituted with serine that should retain the approximate size, geometry, and polarity of the cysteine residues but would be unable to form disulfide bonds. Mutant proteins were purified, analyzed by CD spectroscopy, and tested in the tyrosine phosphorylation assay. Both the far-UV CD spectra (data not shown) and tyrosine phosphorylation (Supplementary Figure 1) were not affected by the mutations, thus indicating that cysteine mutations did not alter the gross conformation of the protein.

Equal amounts of native STAT3 and the mutant proteins were treated with diamide and GSH in a time course experiment (from 1 to 15 min) and analyzed with anti-GSH antibody under non-reducing condition. As shown in Figure 7A, GSH and diamide caused significant S-glutathionylation of both native STAT3 and the single C328S and C542S mutants even after 1 min of treatment. Moreover, the time course analysis showed that S-glutathionylation of the proteins did not change with the time (Figure 7B and C). On the contrary, the STAT3 C328/542S double mutant was found to be more resistant to S-glutathionylation, showing no modification after 1 min and a low extent of S-glutathionylation after 5 min (Figure 7D).

These data suggested that multiple cysteine residues within the STAT3 structure might be involved in a complex redox regulatory mechanism by reversible S-glutathionylation. All mutants, in fact, were phosphorylated by JAK2, showing that cysteine to serine changes did not impair kinase recognition. However, while single mutants were normally modified by GSH, substitutions of the two more susceptible cysteine residues heavily decreased redox regulation. More research is needed to clarify this point and to define the redox-related role of the partially glutathionylated cysteine residues identified in this work.

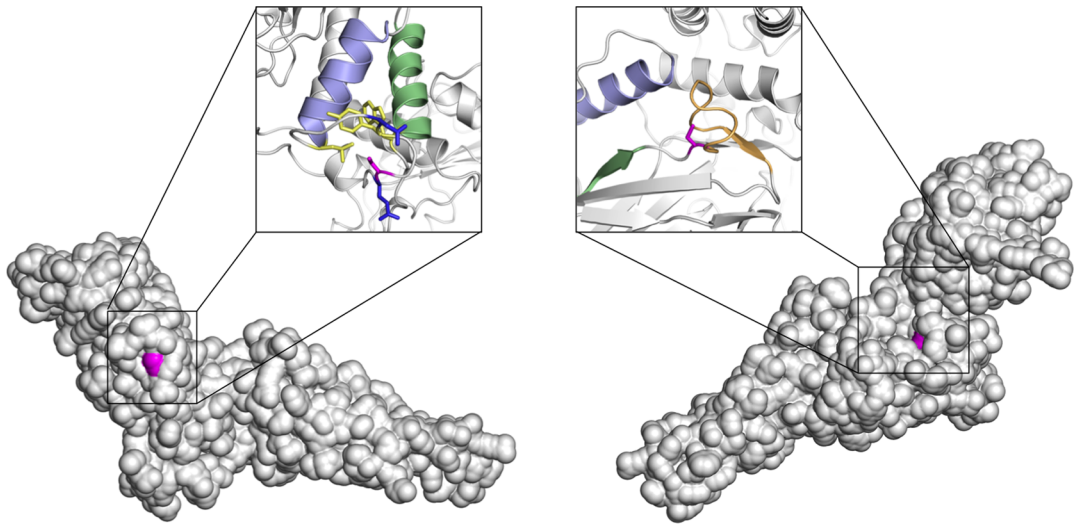

Figure 6. Three-dimensional structure of STAT3 in its monomeric form as obtained by X-ray crystallography (PDB entry: 1BG1). On the left, the structural details of the molecular environment around Cys542 (colored in magenta) are shown. Key residues discussed in the text are represented by sticks, namely, Gln543 and Asn538 are in blue, while the hydrophobic residues Leu533, Tyr539, and Trp501 are in yellow. The two helices, which are expected to slightly dislocate upon glutathionylation of Cys542, are shown in light blue (residues 521−532) and light green (residues 501−515). On the right, the molecular environment around Cys328 (magenta) is shown. The 321−325 strand and a portion of the 198−252 helix are shown in light green and in light blue, respectively, while the 329−340 loop is shown in orange.

dx.doi.org/10.1021/cb500407d | ACS Chem. Biol. 2014, 9, 1885−1893

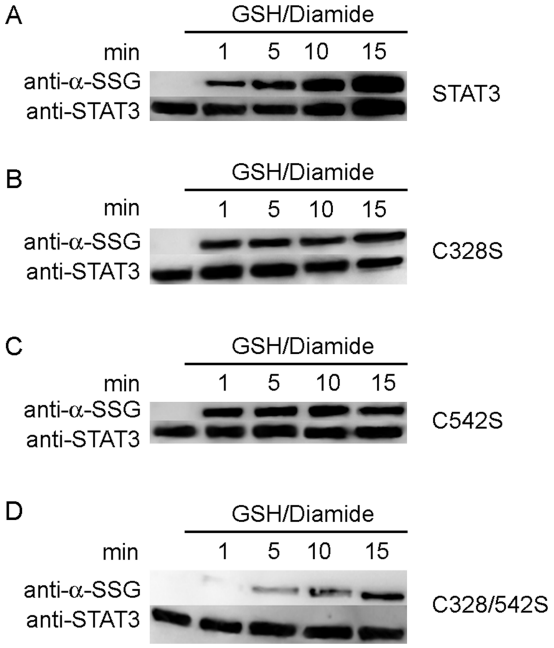

Figure 7. Effect of diamide/GSH treatment on S-glutathionylation of STAT3 mutants. Western blot analysis under non-reducing conditions of S-glutathionylated STAT3 (A), C328S (B), C542S (C), and C338/542S (D) starting from 1 min of diamide/GSH treatment. The blot exhibited equivalent STAT3 levels in all sample The images are representative of 4 independent experiments.

S-Glutathionylation of STAT3 Impairs Its Tyr705 Phosphorylation in HeLa Cells. Recent reports describe regulation of STAT3 Tyr705 phosphorylation via S-glutathionylation under oxidative conditions in different cell lines.[32−34] However, until now, a number of questions remain unanswered with regard to the molecular aspects of STAT3 S-glutathionylation, and it is unclear whether there is more than one cysteine reactive for glutathionylation.

Therefore we investigated redox regulation of STAT3 in a cellular environment using HeLa cells treated with diamide, a membrane-permeable thiol-oxidizing agent that rapidly and reversibly oxidizes GSH to GSSG and promotes formation of protein-glutathione mixed disulfides in cultured cells.[40]

To determine the S-glutathionylation state of STAT3, the protein was immunoprecipitated from cellular extract using anti-STAT3 K-15 antibody and analyzed with anti-GSH antibody under non-reducing condition.

As in other cell lines, 500 μM diamide treatment was able to induce S-glutathionylation of both constitutive and IL-6-activated STAT3 (Figure 8A). Western blot analysis, using anti-pTyr^{705} STAT3 antibody, confirmed that this post-translational modification interfered with the tyrosine phosphorylation state of the protein (Figure 8B). Furthermore, as shown in Figure 8B, the treatment with 1 mM GSSG, another thiol-specific oxidant, inhibited STAT3 Tyr705 phosphorylation to a lesser extent. Western blots exhibited equivalent STAT3 levels in all samples.

As described above, only C328/542S STAT3 was found to be more resistant to S-glutathionylation *in vitro*. In order to analyze the involvement of these cysteines in redox regulation of STAT3 in a cellular environment, HeLa cells were transfected either with wild-type STAT3-pcDNA 3.0 or with C328/542S STAT3-pcDNA 3.0 expression vector. As expected, 500 μM diamide induced S-glutathionylation only in wild-type

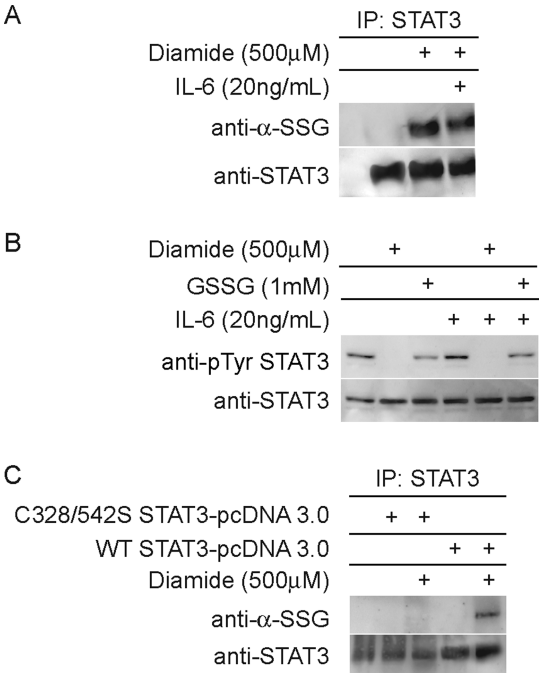

Figure 8. Effect of diamide treatment on S-glutathionylation and phosphorylation of STAT3 in HeLa cells. (A) HeLa cells were treated with 500 μM diamide for 30 min or were pretreated with diamide and then induced with IL-6 (20 ng mL^{-1}) for 15 min. Western blot analysis of immunoprecipitated STAT3 (IP STAT3) shows that diamide induced S-glutathionylation of both constitutive and IL-6 activated STAT3. (B) HeLa cells were treated with 500 μM diamide for 30 min or were pretreated with diamide and then induced with IL-6 (20 ng mL^{-1}) for 15 min. Furthermore cells were treated with 1 mM GSSG for 30 min or were pretreated with GSSG and then induced with IL-6 (20 ng mL^{-1}) for 15 min. Western blot analysis shows that anti-pTyr705 STAT3 antibody was not able to recognize protein after diamide or to a lesser extent GSSG treatment. (C) HeLa cells expressing wild-type or C328/542S STAT3 were treated with 500 μM diamide for 30 min. Western blot analysis of immunoprecipitated STAT3 (IP STAT3) shows that diamide was not able to induce S-glutathionylation of the STAT3 mutant. The blots exhibit equivalent STAT3 levels in all samples. The images are representative of 4 independent experiments.

STAT3-expressing cells and no signal was observed in C328/542S STAT3-expressing cells treated with diamide (Figure 8C).

Conclusion. Modulation of STAT3 phosphorylation by S-glutathionylation suggests a novel mechanism by which oxidative stress regulates STAT3 signaling. Herein we present new data that shed light on the redox status of STAT3, demonstrating that this protein is mainly S-glutathionylated at Cys328 and Cys524. Activated STAT3 may participate in oncogenesis by stimulating cell proliferation and inducing resistance to apoptosis, as well as promoting tumor angiogenesis, invasion, and migration. The tight association of STAT3 activation with transformation and tumor progression makes STAT3 a potential therapeutic target. In this respect, identification of the more sensitive cysteines may have potential implications for new drugs development.

METHODS

Reagents. All chemicals used throughout the present study were of the highest analytical grade, purchased from Sigma, Milan, IT, unless otherwise specified.

dx.doi.org/10.1021/cb500407d | *ACS Chem. Biol.* 2014, 9, 1885−1893

Expression and Purification of Wild-Type and Mutants STAT3. The full-length cDNA coding for human STAT3 (STAT3α) cloned on a pOTB-Stat3 vector was purchased from ImaGENES. STAT3α expression construct coding for amino acid residues 123−723 (STAT3) (Figure 1) was amplified by polymerase chain reaction (PCR) and cloned into the *Sal*I-*Not* I site of the expression vector pGEX4T1 (GE Healthcare). Cys328 to Ser (C328S) and Cys542 to Ser (C542S) mutants were generated by QuikChange site-directed mutagenesis kit (Stratagene) and cloned into the *Sal*I-*Not* I site of the expression vector pGEX4T1. The obtained STAT3 plasmids were transformed into the *E. coli* strain BL21 (DE3, New England BioLab inc). Recombinant clones were verified by DNA sequence analysis. The recombinant proteins were purified by Glutathione Chromatrix (Jena Bioscience) and eluted in 20 mM Tris HCl pH 7.5, 150 mM NaCl (Supporting information).

Glutathionylation Assay *in Vitro*. Wild-type or mutants STAT3 (5 μg mL^{-1}) were incubated at 20 °C for 15 min in 50 mM HEPES pH 7.5 with 125 μM GSH, 125 μM GSSG, or 100 μM diamide alone. Moreover, combined treatments with 125 μM GSH or 125 μM GSSG and 100 μM diamide, were performed. Then, the samples were analyzed by non-reducing SDS-PAGE, and the resolved proteins were electroblotted onto a PVDF membrane (Immobilon P, Millipore, Bedford, MA). The membrane was then blocked by TBS-T containing 3% BSA for 1 h and incubated with the anti-GSH (ViroGen, Watertown, MA) at RT with gentle shaking for 2 h. After washing, the membrane was developed using anti-mouse IgG peroxidase-conjugated antibody (Cell Signaling Technology, Danvers MA, USA) and a chemiluminescent detection system (Immun-Star WesternC Kit, Bio-Rad, Hercules, CA). Blotted proteins were detected and quantified using the ChemiDoc XRS Imaging System (Bio-Rad). After being stripped, the membrane was rehybridized with anti-STAT3 K-15 antibody (Santa Cruz Biotechnology, Santa Cruz, CA) and recognized with anti-rabbit IgG peroxidase-conjugated antibody (Cell Signaling Technology).

MS Analysis of Glutathionylated STAT3. An aliquot of 200 μg of lyophilized recombinant STAT3 was glutathionylated according to the procedure described above. The protein sample was desalted by reversed-phase HPLC on a Phenomenex Jupiter C4 column (250 mm × 2.0 mm, 300 Å pore size) with a linear gradient from 10% to 95% of solvent B (95% acetonitrile in 0.07% TFA) in 30 min, at a flow rate of 200 μL min^{-1} using an Agilent Technologies 1100 HPLC (Agilent Technologies). The eluate was monitored at 220 nm, and the fractions were manually collected and lyophilized.

The main fraction was dissolved in 50 mM ammonium bicarbonate, pH 8.0 and digested with trypsin at 37 °C overnight using an enzyme to substrate ratio of 1:50 w/w. Sample was then acidified with 0.2% TFA and directly analyzed by MALDI-MS onto a 4800 plus MALDI TOF-TOF mass spectrometer (ABI SCIEX) equipped with a reflectron analyzer and used in delayed extraction mode with 4000 Series Explorer v3.5 software. An aliquot of the same peptide mixture was treated with 50 mM DTT in 50 mM ammonium bicarbonate, pH 8.0 at 37 °C for 1 h in order to reduce disulfide bonds. The peptide mixture was then acidified and directly analyzed by MALDI-MS.

For MALDI analyses, 0.5 μL of each peptide mixture was mixed with an equal volume of α-cyano-4-hydroxycynnamic acid as matrix (10 mg mL^{-1} in 0.2% TFA in 70% acetonitrile), loaded onto the metallic sample plate, and air-dried. Mass calibration was performed using the standard mixture provided by the manufacturer. MALDI-MS data were acquired over a 600−5000 m/z mass range in the positive-ion reflector mode. For the MS/MS analyses, specific peaks were selected from MS spectra to perform manual CID experiments, using a 1 kV MS/MS operating mode.

STAT3/JAK2 Kinase Assay *in Vitro*. Purified STAT3 (10 μg) was treated with 125 μM GSH and 100 μM diamide in 1 mM EDTA and 250 mM HEPES pH 7.5 at 20 °C for 15 min. GSH and diamide were removed, and buffer was changed by 3 cycles of concentration−dilution in 20 mM Tris HCl pH 7.5, 150 mM NaCl using a microcentrifugal concentration device with a 30-kDa cutoff membrane (Centricon, Millipore). Afterward, STAT3/JAK2 kinase assay was performed using recombinant JAK2 active protein (Upstate Biotechnology, NY, USA) as described elsewhere with slight modification. Briefly, kinase reactions were performed by incubating 1 μg of STAT3 with 10 ng of JAK2 protein in 30 μL of kinase reaction buffer (20 mM TRIS-HCl, pH 7.5, 50 mM $MgCl_2$, 100 μM ATP). The samples were incubated at 20 °C for 10 min, within the linear reaction range. Reactions were stopped by addition of reducing SDS sample buffer. The samples were then boiled, separated by SDS-PAGE, and immunoblotted with anti-pTyr^{705} STAT3 antibody (Cell Signaling Technology). To verify the autophosphorylation of JAK2, membranes were rehybridized with anti-pTyr$^{1007/1008}$ JAK2 antibody (Millipore). After being stripped the membranes were rehybridized with anti-STAT3 K-15 antibody (Santa Cruz Biotechnology) and anti-JAK2 antibody (Cell Signaling Technology).

Spectroscopic Measurements. Visible and far-UV CD spectra were recorded on a Jasco J-710 spectropolarimeter equipped with a thermostatically controlled compartment at 25 °C, by using 1-cm path length quartz cuvettes. The recombinant STAT3 concentration was 0.5−5 mg mL^{-1}, and the spectra were recorded in 20 mM Tris-HCl pH 7.5. Routinely, three spectra were recorded at a scan speed of 50 nm min^{-1} with a bandwidth of 2 nm and averaged automatically.

Secondary structure content was calculated from far-UV CD spectra using the Dicroweb software.

Intrinsic fluorescence emission spectra were recorded on a Jasco FP-750 spectrofluorometer equipped with a thermostatically controlled cell holder. Spectra of blanks, i.e., samples containing all components except the recombinant STAT3, were taken immediately before the measurements of the samples containing protein. Intrinsic fluorescence spectra (λ_{exc} = 280 nm) were recorded from 300 to 550 nm. For 1-anilino-naphtalene sulfonic acid (ANS) binding studies, protein samples were incubated for 1 h at 25 °C with ANS at a final concentration of 15 μM. Upon excitation at 365 nm, emission spectra were registered from 400 to 600 nm.

Cells Culture. Human cervical carcinoma HeLa cells (American Type Culture Collection) were cultured in DMEM supplemented with 10% FBS, 100 IU mL^{-1} penicillin, 100 μg mL^{-1} streptomycin, and 40 μg mL^{-1} gentamycin in a 5% CO_2 atmosphere at 37 °C.

STAT3 was constitutively expressed in HeLa cells and was hyper-activated after 20 ng mL^{-1} IL-6 administration for 15 min.

Construction of Wild-Type and C328/542S STAT3 Double Mutant. Wild-type (123−723) and C328/542S STAT3 double mutant were amplified by polymerase chain reaction (PCR) and cloned into the *Hind* III-*Not* I site of the expression vector pcDNA 3.0 (Invitrogen, Carlsbad, CA). Recombinant clones were verified by the DNA sequence analysis.

Cells Transfection. For transient transfection, HeLa cells were plated into 60 mm plates at a density of 8 × 10^5 cells in DMEM without antibiotics. After 18 h, the DMEM was replaced with the serum-reduced medium OPTI-MEM (Invitrogen), and the cells were transfected with 1.5 μg of wild-type STAT3-pcDNA 3.0 or with 1.5 μg of C328/542S STAT3-pcDNA 3.0 expression vector and 6 μL of Lipofectamine 2000 according to the manufacturer's instructions (Invitrogen). After 24 h, the cells were treated with 500 μM diamide for 30 min. The cells were harvested and used for analysis of S-glutathionylation of STAT3 by immunoprecipitation.

Analysis of S-Glutathionylated STAT3 in HeLa Cells. Cells were lysed at 4 °C in RIPA buffer (20 mM Tris HCl, pH 8.0, 150 mM NaCl, 1% Nonidet P-40, 1 mM EDTA, 10% glycerol, 100 mM NaF, 1 mM Na_3VO_4) supplemented with protease cocktail inhibitor for 15 min with occasional vortexing. Equal amounts of proteins from the clarified cell lysates were incubated overnight at 4 °C with rotation in the presence of 4 μg of anti-STAT3 K-15 antibody (Santa Cruz Biotechnology). The immune complexes were collected by addition of protein A sepharose (Millipore), extensively washed, eluted in a non-reducing sample buffer (62.5 mM Tris HCl, pH 6.8, 10% glycerol, 5% SDS, 0.05% bromophenol blue), and separated by SDS-PAGE. After electrophoresis, proteins were transferred to a PVDF membrane. The membrane was then probed with anti-GSH or anti-STAT3 K-15 antibodies as previously described.

Analysis of Tyr705 Phosphorylated STAT3 in HeLa Cells. Cells were homogenized at 4 °C in 20 mM HEPES, pH 7.4, containing

420 mM NaCl, 1 mM EDTA, 1 mM EGTA, 1% Nonidet-P40, 20% glycerol, protease cocktail inhibitors, and phosphatase cocktail inhibitors. An aliquot of the cell lysates (50 μg total protein/lane) was separated by SDS-PAGE and immunoblotted with anti-pTyr^{705} STAT3 antibody as previously described. After being stripped, the membrane was rehybridized with anti-STAT3 K-15 antibody.

■ ASSOCIATED CONTENT

Supporting Information

This material is available free of charge via the Internet at http://pubs.acs.org.

■ AUTHOR INFORMATION

Corresponding Author

*E-mail: sofia.mariotto@univr.it.

Notes

The authors declare no competing financial interest.

■ ACKNOWLEDGMENTS

This work was supported by funds from the Italian Ministry for Research and Education (FUR2011MS and FUR2012MS) and F.A.R.O. Grant 2011, University of Naples and Compagnia di San Paolo.

■ REFERENCES

(1) Heinrich, P. C., Behrmann, I., Muller-Newen, G., Schaper, F., and Graeve, L. (1998) Interleukin-6-type cytokine signalling through the gp130/Jak/STAT pathway. *Biochem. J. 334* (Pt 2), 297−314.

(2) Nagata, Y., and Todokoro, K. (1996) Interleukin 3 activates not only JAK2 and STAT5, but also Tyk2, STAT1, and STAT3. *Biochem. Biophys. Res. Commun. 221*, 785−789.

(3) Shuai, K., and Liu, B. (2003) Regulation of JAK-STAT signalling in the immune system. *Nat. Rev. Immunol. 3*, 900−911.

(4) Benekli, M., Baumann, H., and Wetzler, M. (2009) Targeting signal transducer and activator of transcription signaling pathway in leukemias. *J. Clin. Oncol. 27*, 4422−4432.

(5) Darnell, J. E., Jr. (1997) STATs and gene regulation. *Science 277*, 1630−1635.

(6) Zhong, Z., Wen, Z., and Darnell, J. E., Jr. (1994) Stat3: a STAT family member activated by tyrosine phosphorylation in response to epidermal growth factor and interleukin-6. *Science 264*, 95−98.

(7) Johnston, P. A., and Grandis, J. R. (2011) STAT3 signaling: anticancer strategies and challenges. *Mol. Interventions 11*, 18−26.

(8) Kamimura, D., Ishihara, K., and Hirano, T. (2003) IL-6 signal transduction and its physiological roles: the signal orchestration model. *Rev. Physiol. Biochem. Pharmacol. 149*, 1−38.

(9) Bournazou, E., and Bromberg, J. (2013) Targeting the tumor microenvironment: JAK-STAT3 signaling. *JAKSTAT 2*, e23828.

(10) Danese, S., and Mantovani, A. (2010) Inflammatory bowel disease and intestinal cancer: a paradigm of the Yin-Yang interplay between inflammation and cancer. *Oncogene 29*, 3313−3323.

(11) Atreya, R., and Neurath, M. F. (2008) Signaling molecules: the pathogenic role of the IL-6/STAT-3 trans signaling pathway in intestinal inflammation and in colonic cancer. *Curr. Drug Targets 9*, 369−374.

(12) Mariotto, S., Esposito, E., Di Paola, R., Ciampa, A., Mazzon, E., de Prati, A. C., Darra, E., Vincenzi, S., Cucinotta, G., Caminiti, R., Suzuki, H., and Cuzzocrea, S. (2008) Protective effect of Arbutus unedo aqueous extract in carrageenan-induced lung inflammation in mice. *Pharmacol. Res. 57*, 110−124.

(13) Andres, R. M., Paya, M., Montesinos, M. C., Ubeda, A., Navalon, P., Herrero, M., Verges, J., and Terencio, M. C. (2013) Potential antipsoriatic effect of chondroitin sulfate through inhibition of NF-kappaB and STAT3 in human keratinocytes. *Pharmacol. Res. 70*, 20−26.

(14) Toffanin, S., Friedman, S. L., and Llovet, J. M. (2010) Obesity, inflammatory signaling, and hepatocellular carcinoma-an enlarging link. *Cancer Cell 17*, 115−117.

(15) Turkson, J., and Jove, R. (2000) STAT proteins: novel molecular targets for cancer drug discovery. *Oncogene 19*, 6613−6626.

(16) Yu, H., Pardoll, D., and Jove, R. (2009) STATs in cancer inflammation and immunity: a leading role for STAT3. *Nat. Rev. Cancer 9*, 798−809.

(17) Darnell, J. E. (2005) Validating Stat3 in cancer therapy. *Nat. Med. 11*, 595−596.

(18) Qu, Y., Oyan, A. M., Liu, R., Hua, Y., Zhang, J., Hovland, R., Popa, M., Liu, X., Brokstad, K. A., Simon, R., Molven, A., Lin, B., Zhang, W. D., McCormack, E., Kalland, K. H., and Ke, X. S. (2013) Generation of prostate tumor-initiating cells is associated with elevation of reactive oxygen species and IL-6/STAT3 signaling. *Cancer Res. 73*, 7090−7100.

(19) Duan, W., Yang, Y., Yi, W., Yan, J., Liang, Z., Wang, N., Li, Y., Chen, W., Yu, S., Jin, Z., and Yi, D. (2013) New role of JAK2/STAT3 signaling in endothelial cell oxidative stress injury and protective effect of melatonin. *PLoS One 8*, e57941.

(20) Maziere, C., Alimardani, G., Dantin, F., Dubois, F., Conte, M. A., and Maziere, J. C. (1999) Oxidized LDL activates STAT1 and STAT3 transcription factors: possible involvement of reactive oxygen species. *FEBS Lett. 448*, 49−52.

(21) Carballo, M., Conde, M., El Bekay, R., Martin-Nieto, J., Camacho, M. J., Monteseirin, J., Conde, J., Bedoya, F. J., and Sobrino, F. (1999) Oxidative stress triggers STAT3 tyrosine phosphorylation and nuclear translocation in human lymphocytes. *J. Biol. Chem. 274*, 17580−17586.

(22) Li, L., Cheung, S. H., Evans, E. L., and Shaw, P. E. (2010) Modulation of gene expression and tumor cell growth by redox modification of STAT3. *Cancer Res. 70*, 8222−8232.

(23) Kim, J., Won, J. S., Singh, A. K., Sharma, A. K., and Singh, I. (2013) STAT3 regulation by S-nitrosylation: Implication for inflammatory disease. *Antioxid. Redox. Signal. 20*, 2514−2527.

(24) Zgheib, C., Kurdi, M., Zouein, F. A., Gunter, B. W., Stanley, B. A., Zgheib, J., Romero, D. G., King, S. B., Paolocci, N., and Booz, G. W. (2012) Acyloxy nitroso compounds inhibit LIF signaling in endothelial cells and cardiac myocytes: evidence that STAT3 signaling is redox-sensitive. *PLoS One 7*, e43313.

(25) Poole, L. B. (2004) Formation and functions of protein sulfenic acids. *Curr. Protoc. Toxicol.*, DOI: 10.1002/0471140856.tx1701s18.

(26) Dalle-Donne, I., Rossi, R., Colombo, G., Giustarini, D., and Milzani, A. (2009) Protein S-glutathionylation: a regulatory device from bacteria to humans. *Trends Biochem. Sci. 34*, 85−96.

(27) Rehder, D. S., and Borges, C. R. (2010) Cysteine sulfenic acid as an intermediate in disulfide bond formation and nonenzymatic protein folding. *Biochemistry 49*, 7748−7755.

(28) Mieyal, J. J., Gallogly, M. M., Qanungo, S., Sabens, E. A., and Shelton, M. D. (2008) Molecular mechanisms and clinical implications of reversible protein S-glutathionylation. *Antioxid Redox Signaling 10*, 1941−1988.

(29) Sitia, R., and Molteni, S. N. (2004) Stress, protein (mis)folding, and signaling: the redox connection. *Sci. STKE 2004*, pe27.

(30) Held, J. M., and Gibson, B. W. (2012) Regulatory control or oxidative damage? Proteomic approaches to interrogate the role of cysteine oxidation status in biological processes. *Mol. Cell Proteomics 11*, R111 013037.

(31) Winterbourn, C. C., and Hampton, M. B. (2008) Thiol chemistry and specificity in redox signaling. *Free Radical Biol. Med. 45*, 549−561.

(32) Xie, Y., Kole, S., Precht, P., Pazin, M. J., and Bernier, M. (2009) S-glutathionylation impairs signal transducer and activator of transcription 3 activation and signaling. *Endocrinology 150*, 1122−1131.

(33) Butturini, E., Cavalieri, E., de Prati, A. C., Darra, E., Rigo, A., Shoji, K., Murayama, N., Yamazaki, H., Watanabe, Y., Suzuki, H., and Mariotto, S. (2011) Two naturally occurring terpenes, dehydrocostuslactone and costunolide, decrease intracellular GSH content and inhibit STAT3 activation. *PLoS One 6*, e20174.

(34) Butturini, E., Carcereri de Prati, A., Chiavegato, G., Rigo, A., Cavalieri, E., Darra, E., and Mariotto, S. (2013) Mild oxidative stress induces S-glutathionylation of STAT3 and enhances chemosensitivity of tumoural cells to chemotherapeutic drugs. *Free Radical Biol. Med. 65C*, 1322−1330.
(35) Ghezzi, P. (2013) Protein glutathionylation in health and disease. *Biochim. Biophys. Acta 1830*, 3165−3172.
(36) Nkansah, E., Shah, R., Collie, G. W., Parkinson, G. N., Palmer, J., Rahman, K. M., Bui, T. T., Drake, A. F., Husby, J., Neidle, S., Zinzalla, G., Thurston, D. E., and Wilderspin, A. F. (2013) Observation of unphosphorylated STAT3 core protein binding to target dsDNA by PEMSA and X-ray crystallography. *FEBS Lett. 587*, 833−839.
(37) Dalle-Donne, I., Milzani, A., Gagliano, N., Colombo, R., Giustarini, D., and Rossi, R. (2008) Molecular mechanisms and potential clinical significance of S-glutathionylation. *Antioxid. Redox Signaling 10*, 445−473.
(38) Starke, D. W., Chock, P. B., and Mieyal, J. J. (2003) Glutathione-thiyl radical scavenging and transferase properties of human glutaredoxin (thioltransferase). Potential role in redox signal transduction. *J. Biol. Chem. 278*, 14607−14613.
(39) Becker, S., Groner, B., and Muller, C. W. (1998) Three-dimensional structure of the Stat3beta homodimer bound to DNA. *Nature 394*, 145−151.
(40) Lock, J. T., Sinkins, W. G., and Schilling, W. P. (2011) Effect of protein S-glutathionylation on Ca2+ homeostasis in cultured aortic endothelial cells. *Am. J. Physiol. Heart Circ. Physiol. 300*, H493−506.